Articles

Phase Polymorphism, Molecular Interactions, and Miscibility of Binary Mixtures of Dimyristoyl-*N*-biotinylphosphatidylethanolamine with Dimyristoylphosphatidylcholine

Musti J. Swamy,[‡,§] Ulrich Würz,[||] and Derek Marsh*[,‡]

Abteilungen Spektroskopie und Kinetik der Phasenbildung, Max-Planck-Institut für biophysikalische Chemie, D-37077 Göttingen, Federal Republic of Germany

Received February 3, 1995; Revised Manuscript Received April 7, 1995[⊗]

ABSTRACT: The phase diagram of hydrated binary mixtures of dimyristoyl-*N*-biotinylphosphatidylethanolamine with dimyristoylphosphatidylcholine in 1 M NaCl has been established by differential scanning calorimetry. Identification of the structures of the phases involved has been made by using X-ray diffraction, spin label ESR spectroscopy, and ^{31}P NMR spectroscopy. On the composition axis, the phase diagram is divided into three regions corresponding to formation of compounds in the gel phase with biotinyl lipid to phosphatidylcholine stoichiometries of approximately 1:1 and 1:3 mol/mol. For the first two regions (up to 75 mol % phosphatidylcholine), the lipids in the gel phase have interdigitated chains (L_{β}^{i}), whereas in the third region the gel phase is not interdigitated ($L_{\beta'}$ or L_{β}). For the first region (up to 50 mol % phosphatidylcholine), the fluid phase is of the novel isotropic type (I_{M_I}) composed of aggregated normal micelles that is characteristic of shorter chainlength biotinylated lipids [Swamy, M. J., Würz, U., & Marsh, D. (1993) *Biochemistry 32*, 9960−9967], whereas for the other two regions a normal fluid lamellar (L_{α}) phase obtains. The equimolar mixture, which lies at a stoichiometric phase boundary, melts isothermally and then undergoes a transition from the isotropic I_{M_I} structure to the lamellar L_{α} structure with increasing temperature in the fluid phase.

Ethanolamine phospholipids that are derivatized at their polar group with the vitamin biotin are capable of binding the proteins avidin and streptavidin with high affinity (Wilchek & Bayer, 1989). This property is not only relevant as a model for recognition and specific protein−lipid interaction at cell membrane surfaces (Swamy & Marsh, 1993) but also of practical application in cytological localization (Bayer et al., 1979), liposome targetting (Urdal & Hakamori, 1980), and the formation of ordered arrays for high-resolution structure determinations (Darst et al., 1991).

In previous studies, it has been demonstrated that aqueous dispersions of biotinylphosphatidylethanolamines display a rich structural polymorphism (Swamy et al., 1994; Swamy & Marsh, 1994). This extends not only to the less common phases, such as those with interdigitated chains, that are displayed by normal membrane phospholipids but also, depending on chain length, to a novel isotropic phase, the I_{M_I} phase, that so far is unique to *N*-biotinylphosphatidylethanolamines (Swamy et al., 1993). For all the above-mentioned applications, the interactions of biotinylated lipids with membrane lipids will play an important role. Parameters such as miscibility, molecular compound formation, phase transitions and separations, in addition to the formation of nonlamellar phases, are likely to be of direct relevance.

The classical and established approach to the study of such aspects of lipid behavior lies in the construction of binary phase diagrams (Cevc & Marsh, 1987). In the present work, we have determined the phase diagram for mixtures of a biotinyl lipid, dimyristoyl-*N*-biotinylphosphatidylethanolamine (DMBPE),[1] with the membrane lipid dimyristoylphosphatidylcholine (DMPC) by using differential scanning calorimetry. The structures of the fluid and gel phases of the various mixtures have been established by using X-ray diffraction, spin label ESR spectroscopy, and ^{31}P NMR spectroscopy. Although the chain lengths of the two lipids are identical, the phase diagram of their mixtures is found to be surprisingly complex, including the formation of two stoichiometric complexes in the gel phase. In addition, the mixtures display the full range of polymorphic states that are characteristic of the biotinyl lipids alone, and one of the isothermally melting compounds undergoes a further structural transition in the fluid phase.

* Author to whom correspondence should be addressed.
‡ Abteilung Spektroskopie.
§ Present address: School of Chemistry, University of Hyderabad, Central University P.O., Hyderabad-500 134, India.
|| Abteilung Kinetik der Phasenbildung.
⊗ Abstract published in *Advance ACS Abstracts,* May 15, 1995.

[1] Abbreviations: biotin-PE, *N*-biotinylphosphatidylethanolamine; DMBPE, 1,2-dimyristoyl-*sn*-glycero-3-(*N*-biotinyl)phosphoethanolamine; DMPC, 1,2-dimyristoyl-*sn*-glycero-3-phosphocholine; n-PCSL, 1-acyl-2-[*n*-(4,4-dimethyloxazolidine-*N*-oxyl)stearoyl]-*sn*-glycero-3-phosphocholine; EDTA, ethylenediaminetetraacetic acid; Hepes, *N*-(2-hydroxyethyl)piperazine-*N'*-2-ethanesulfonic acid; NMR, nuclear magnetic resonance; ESR, electron spin resonance; L_{β}^{i}, lamellar gel phase with interdigitated chains; L_{β}, lamellar gel phase with untilted and noninterdigitated chains; L_{α}, fluid lamellar phase; I_{M_I}, fluid isotropic phase composed of aggregated normal micelles.

0006-2960/95/0434-7295$09.00/0

MATERIALS AND METHODS

Materials. Dimyristoylphosphatidylcholine and dimyristoylphosphatidylethanolamine were obtained from Fluka (Buchs, Switzerland). *N*-biotinylated dimyristoylphosphatidylethanolamine, DMBPE, was synthesized from dimyristoylphosphatidylethanolamine and biotinyl-*N*-hydroxysuccinimide (Sigma, St. Louis, MO) according to Bayer et al. (1979). Phospholipid spin labels (5-PCSL and 14-PCSL) were synthesized as described in Marsh and Watts (1982).

Sample Preparation. Samples for ^{31}P NMR spectroscopy were prepared by codissolving 20−40 mg of the required lipid mixture (DMPC + DMBPE) in dichloromethane, removing the solvent by rotary evaporation, and drying overnight under vacuum. The dry lipid was hydrated with 0.5 mL of 1 M NaCl, 10 mM Hepes, and 1 mM EDTA, pH 7.4 buffer at approximately 10 °C above the chain-melting temperature and transferred to a 10 mm NMR tube. Samples were freeze-thawed five times before measurement. The samples were then pelleted in a bench top centrifuge, and excess buffer was removed prior to measurement.

Samples for ESR spectroscopy were prepared by codissolving 1 mg of lipid and 1 mol % of the 5-PCSL or 14-PCSL spin label in dichloromethane. The dried lipid was hydrated with 200 μL of buffer (cf. above) and pelleted in a glass capillary of 1 mm diameter. Excess supernatant was removed before sealing the capillary.

For X-ray diffraction measurements, either an aliquot of the samples prepared for NMR measurements or a smaller sample prepared in an equivalent manner was transferred to a 1 mm diameter fine-wall glass capillary and centrifuged at 3000 rpm in a bench top centrifuge for ca. 5 min, and the excess supernatant was removed. The capillary was then flame sealed.

Differential Scanning Calorimetry. Differential scanning calorimetry was performed with a Model 4207 heat-flow calorimeter from Hart Scientific. Samples, prepared as above, consisted of 2−4 mg of the lipid mixture dispersed in 0.5 mL of buffer, and scan rates were 5 °C per h. An empty reference cell was used and baseline correction was made with a blank buffer sample. Transition enthalpies were evaluated by using the peak integration software supplied with the instrument together with the measured value of the scan rate at the point of the transition. Lipid concentrations were determined by phosphate assay (Rouser et al., 1970).

Electron Spin Resonance Spectroscopy. ESR spectra were recorded on a Varian E-12 Century Line 9 GHz spectrometer equipped with nitrogen gas flow temperature regulation. Samples were contained in sealed 1 mm ID glass capillaries accommodated within a standard quartz ESR tube which contained silicone oil for thermal stability. Temperature was measured with a thermocouple situated in the silicone oil just above the top of the ESR cavity.

X-ray Diffraction. X-ray diffraction measurements were performed using a Kratky small-angle X-ray scattering apparatus with slit geometry [see Würz (1988)]. Compared with the range of scattering angles covered, the slit can be regarded as of infinite length, and the half-width of the beam (1.5×10^{-3} Å^{-1}) is negligible. Sample capillaries were mounted in a massive copper housing which was thermostated with a Peltier device. Temperature stability and gradients were better than 0.1 K. Nickel-filtered Cu Kα radiation ($\lambda = 0.154$ nm) was obtained from an AEG fine-focus tube, and diffracted intensity was recorded with a linear position-sensitive detector mounted on an extension tube at a distance of 98.35 cm from the sample. To record data at higher scattering angles, the detector was repositioned in a direction orthogonal to the beam. Diffraction patterns are presented as scattering intensity that has not been corrected for the slit geometry.

^{31}P Nuclear Magnetic Resonance Spectroscopy. Proton-dipolar decoupled ^{31}P NMR spectra were recorded at a frequency of 121.5 MHz on a Bruker MSL-300 spectrometer operating in the Fourier transform mode. The $\pi/2$ pulse width was 11 μs, and recycle delays were always in excess of $5T_1$. The decoupling power was approximately 10−15 W, and the duty cycle of the gated decoupling was ca. 0.2%. Temperature was regulated by a thermostated nitrogen gas flow system.

RESULTS AND DISCUSSION

The molecular interactions between the biotin lipid and phosphatidylcholine of the same chain composition are characterized first by using differential scanning calorimetry. Then the various structures that the lipid mixtures assume are characterized in terms of the novel phases already established for biotinylated phosphatidylethanolamines alone (Swamy et al., 1993) and the normal bilayer membrane phases typical of phosphatidylcholines. Experiments were performed in 1 M NaCl to suppress electrostatic effects and because under these conditions biotinylated phosphatidylethanolamines express their richest phase behavior.

Differential Scanning Calorimetry. The DSC thermograms of various hydrated binary mixtures of dimyristoyl-*N*-biotinylphosphatidylethanolamine with dimyristoylphosphatidylcholine are given in Figures 1 and 2 for heating scans and cooling scans, respectively. These are characterized by a multivariate response with progressively increasing DMPC content. An admixture of DMPC initially results in a relatively broad transition region, the temperature of the upper boundary of which increases rapidly with increasing DMPC content. This reaches a maximum for the 1:1 mol/mol mixture, at which composition the transition is rather sharp indicating the formation of an isothermally melting compound. Beyond this, the transition region first decreases in temperature reaching a minimum for mixtures with approximately 1:3 mol/mol DMBPE/DMPC stoichiometry. Again, the 1:3 mol/mol mixture exhibits a sharp transition characteristic of an isothermally melting compound. The transition region then subsequently increases in temperature up to the gel-to-fluid transition temperature of DMPC. The behavior in heating and cooling scans is broadly similar, except that the exotherms for the 60:40 and 70:30 mol/mol DMPC/DMBPE mixtures exhibit two peaks. The reason for this most likely is that, on cooling, a transition takes place first to a metastable noninterdigitated gel phase and that this then subsequently converts to the stable interdigitated gel phase (cf. later). Consistent with this, the higher temperature peak for the 60:40 mol/mol mixture has an enthalpy close to that for DMPC alone (which forms a noninterdigitated gel phase), whereas the total enthalpy of both peaks is similar to that for the single peak that is obtained in the heating scans. A similar interpretation has been given for the calorimetric behavior of phosphatidylcholines in glycerol which also form interdigitated gel phases (Boggs & Rangaraj, 1985).

The calorimetrically determined enthalpies obtained from integration of the excess heat capacities in the transition

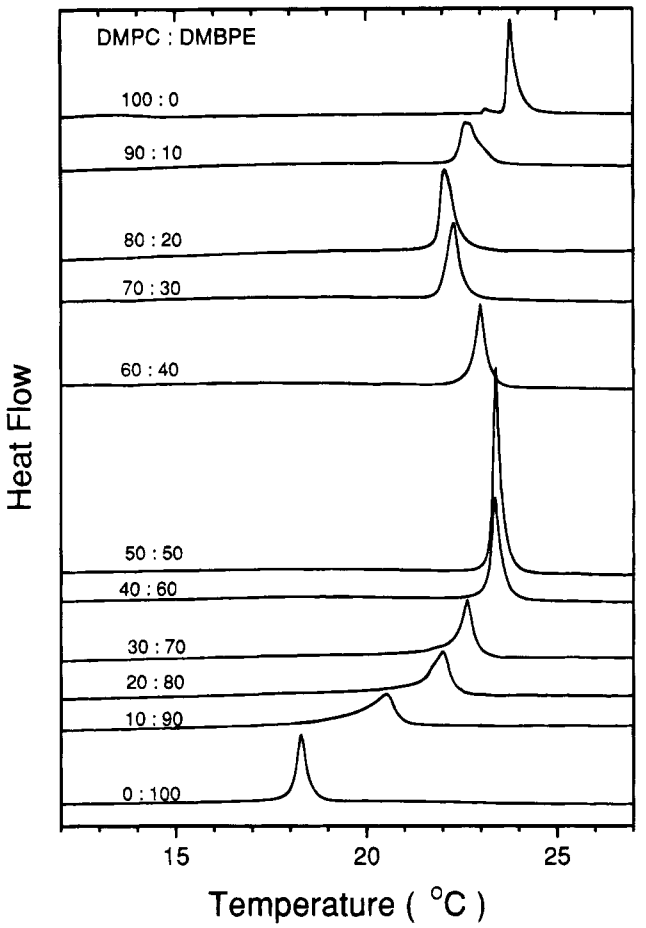

FIGURE 1: Differential scanning calorigrams from DMPC/DMBPE binary mixtures dispersed at a concentration of 4−5 mg/mL in 1 M NaCl, 10 mM Hepes, and 1 mM EDTA, pH 7.4, recorded at a heating rate of 5 °C per h. The composition of the lipid mixtures (in mole ratio) is indicated on the figure.

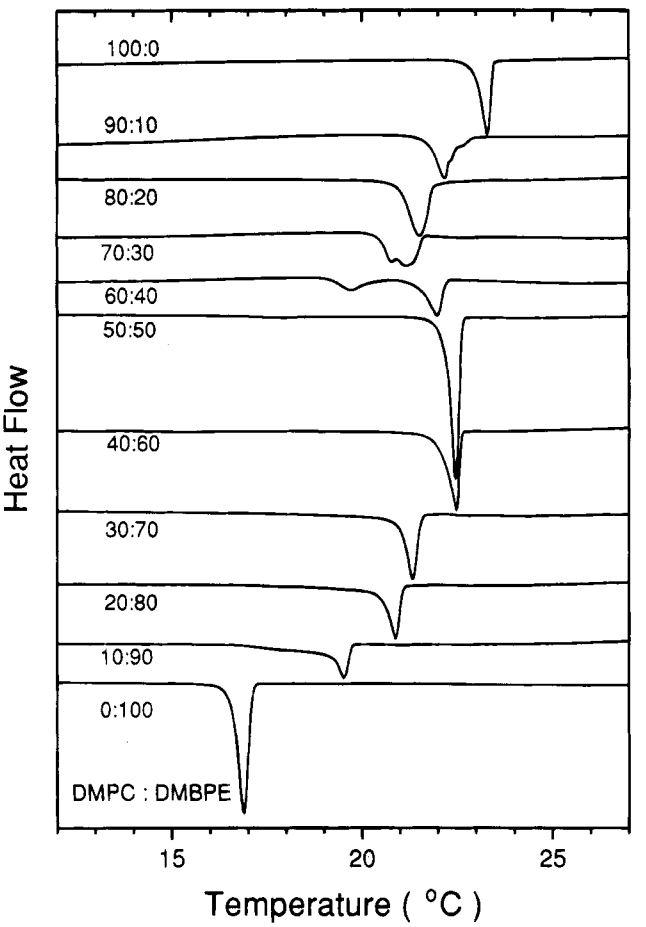

FIGURE 2: Differential scanning calorigrams from DMPC/DMBPE binary mixtures dispersed at a concentration of 4−5 mg/mL in 1 M NaCl, 10 mM Hepes, and 1 mM EDTA, pH 7.4, recorded at a cooling rate of 5 °C per h. The composition of the lipid mixtures (in mole ratio) is indicated on the figure.

regions are given in Table 1, along with the approximate widths of the corresponding transition regions. The enthalpies measured from heating scans were similar to those measured from cooling scans. The data given in Table 1 are the average for heating and cooling. In general, the enthalpies remain approximately constant (≈8−8.5 kcal/mol) with increasing DMPC content, up to the equimolar mixture. Beyond this, the enthalpy drops to the value characteristic of the gel-to-fluid transition of DMPC, with a minor local maximum at 80 mol % DMPC.

Binary Phase Diagram. Temperature−composition binary phase diagrams derived from the calorimetric data in Figures 1 and 2 are given in Figure 3, for both heating and cooling scans. The phase diagram divides rather clearly into three separate regions along the composition axis, reflecting the trends already noted for the DSC thermograms. In accordance with the phase rule, this behavior corresponds to the formation of stoichiometric compounds in the lipid gel phase. One of these corresponds to the isothermal melting behavior at approximately 1:1 mol/mol lipid admixture (compound C1), and the other to a DMBPE/DMPC stoichiometry of 1:3 mol/mol (compound C2).

In the first region of the phase diagram, the gel phase consists of a mixture of DMBPE with the high-melting compound C1. The transition temperatures of these two differ significantly, and they exhibit a considerable degree of gel-phase immiscibility that is particularly evident from the data obtained on cooling. Correspondingly, the region

Table 1: Calorimetric Enthalpies, ΔH (Mean of Heating and Cooling), for DMBPE/DMPC Binary Mixtures Dispersed in 1 M NaCl, 10 mM Hepes, and 1 mM EDTA, pH 7.4[a]

DMPC/DMBPE (mol/mol)	ΔT (°C)	ΔH (kcal/mol)	DMPC/DMBPE (mol/mol)	ΔT (°C)	ΔH (kcal/mol)
100:0	0.5	5.1	40:60	0.5	8.2
90:10	1.3	5.0	30:70	1.6	8.3
80:20	1.1	6.5	33:67	1.7	7.4
75:25	0.8	6.1	20:80	3.4	8.6
70:30	1.0	5.8	10:90	3.2	8.4
60:40	0.8	6.8	0:100	0.7	8.1
50:50	0.5	7.9			

[a] ΔT is the width of the phase separation region (heating scans).

of gel−fluid phase coexistence is relatively broad. In the second region, the gel phase corresponds to a mixture of the high-melting compound C1 with the low-melting compound C2. The transition temperatures of these compounds are rather similar, they exhibit gel-phase miscibility, and the region of gel−fluid coexistence is relatively narrow. In the third region, the gel phase contains a mixture of compound C2 with DMPC, both of which have rather similar transition temperatures and therefore the phase behavior is thermodynamically rather similar to that in the second region of the phase diagram. All regions of the phase diagram are indicative of at least partial, if not full, miscibility in the fluid phase.

X-ray Diffraction. To obtain information on the structures of the lipid assemblies in the various gel and fluid regions

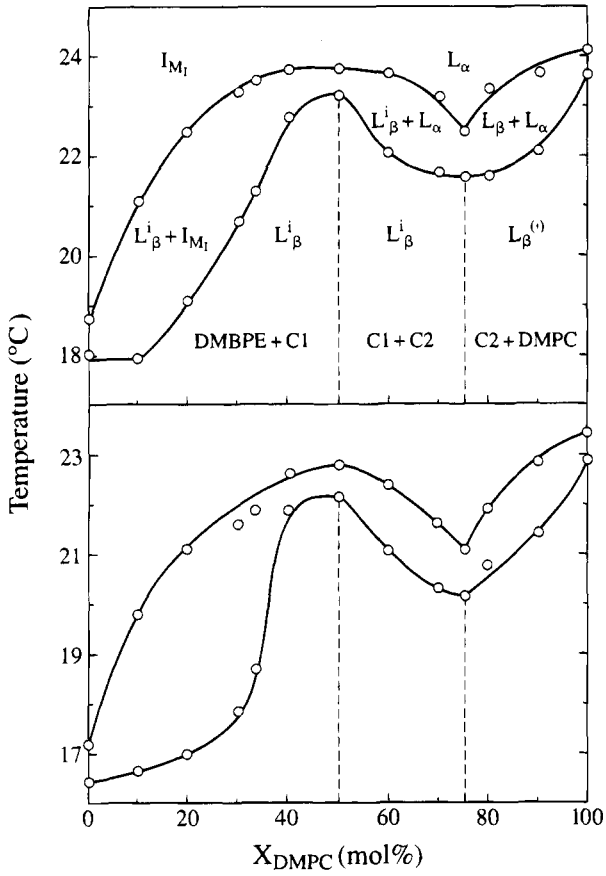

FIGURE 3: Binary phase diagram of DMPC/DMBPE mixtures hydrated in 1 M NaCl, 10 mM Hepes, and 1 mM EDTA, pH 7.4, deduced from the phase boundaries established from (upper) the DSC endotherms in Figure 1 and (lower) the DSC exotherms of Figure 2. The solidus and liquidus points were determined from the onset and completion of the change in excess heat capacity, respectively. The characterization of the structures indicated for the phases is given later. C1 and C2 are compounds with approximate DMBPE/DMPC stoichiometries of 1:1 and 1:3 mol/mol, respectively, as indicated by the vertical dashed lines.

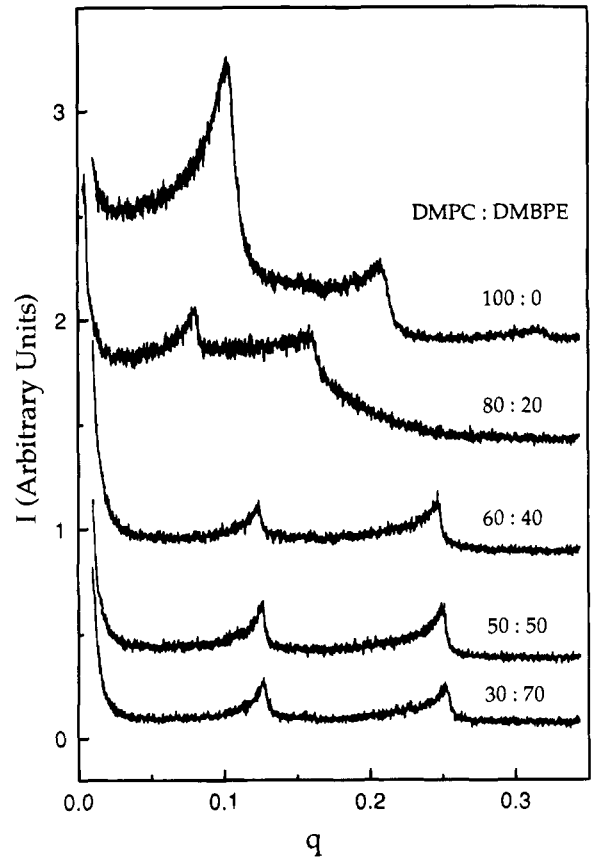

FIGURE 4: Small-angle X-ray diffraction patterns of DMPC/DMBPE binary mixtures hydrated in excess 1 M NaCl, 10 mM Hepes, and 1 mM EDTA, pH 7.4, recorded at 10 °C in the gel phase. The magnitude of the scattering vector, q (Å^{-1}), is $2\pi \sin 2\theta/\lambda$, where 2θ is the scattering angle. The composition of the lipid mixtures (in mole ratio) is indicated on the figure.

of the phase diagram, x-ray diffraction studies were performed. The small-angle diffraction patterns obtained from the lipid mixtures in the gel and fluid phases are given in Figures 4 and 5, respectively.

In the gel phase, at 10 °C, two or three orders of diffraction are observed that correspond to the repeat spacings of lamellar structures, the values of which are given in Table 2. For mixtures with 40 mol % DMBPE or higher (corresponding to the first two regions of the phase diagram in Figure 3), the repeat spacings are rather similar. The values are all considerably smaller than that for DMPC, which is known to have strongly tilted, but noninterdigitated, chains in the gel phase [i.e., $L_{\beta'}$ (Janiak et al., 1976)]. Because of this, and the similarity with the repeat spacing of DMBPE alone (cf. Table 2) that has an interdigitated gel phase (Swamy et al., 1993), it seems most probable that the gel phase in the first two regions of the phase diagram is of the interdigitated $L_\beta{}^i$-type. A change in thickness of the intervening water layers, however, cannot be excluded entirely. Further support for the suggestion of an interdigitated gel phase in the first two regions of the phase diagram comes from the unusually high intensity of the second-order reflections, which is not normally a feature of noninterdigitated lamellar phases (cf. DMPC alone in Figures 4 and 5). In spite of the, at least partial, gel phase immiscibility in the first region of the phase diagram, only a single diffraction pattern is observed, suggesting that the interdigitated gel phases of DMBPE and of the compound C1 have rather similar long spacings. For the mixture containing 20 mol % DMBPE (corresponding to the third region of the phase diagram in Figure 3), the long spacing is considerably larger than that for DMPC gel-phase bilayers. It is therefore extremely unlikely that the lipid chains are interdigitated in the gel phase for this region of the phase diagram. The large repeat spacing could be caused partly by the larger bulk of the DMBPE polar headgroup, which also might be responsible for a change in the extent of hydration, and additionally its interaction with DMPC might cause a decrease in the degree of tilt of the lipid chains.

In the fluid phase, at 30 °C, sharp lamellar diffractions, which are characteristic for DMPC bilayers, are not observed in all cases. Already for the mixture with 20 mol % DMBPE, the second diffraction order is rather broad, suggesting a loss of coherence between the multilamellae and possibly a distribution of interlamellar spacings. For the mixture with 40 mol % DMBPE, a sharp first-order reflection is still observed, superimposed on a broad background scatter. From this, it can be concluded that the fluid phase is lamellar in the second and third regions of the phase diagram given in Figure 3, although the behavior may be more complex in the second region. The lamellar repeat spacings are given in Table 2. An increase in spacing is observed on adding DMBPE, paralleling the results already discussed for the gel phase. At 50 mol % DMBPE and above, a broad continuous scatter is observed from the mixtures that is very similar to that found previously for

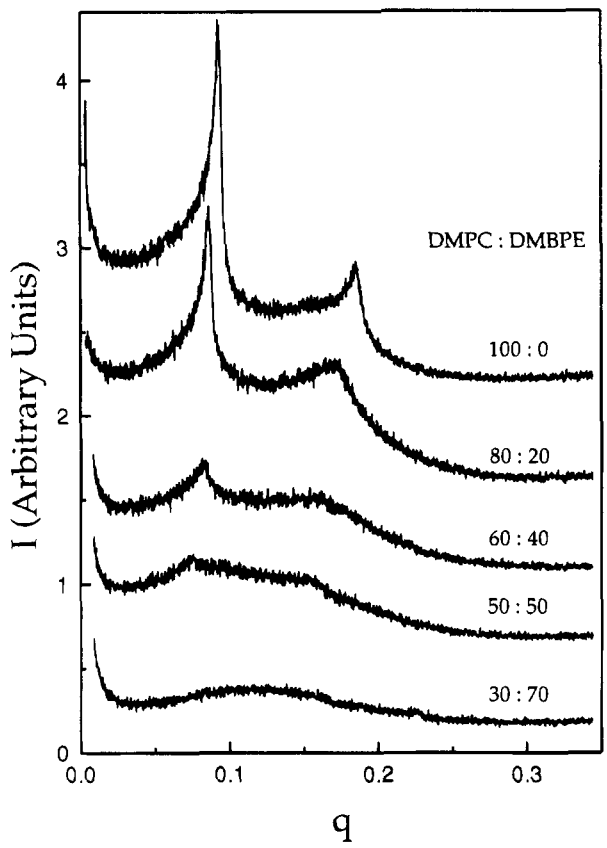

FIGURE 5: Small-angle X-ray diffraction patterns of DMPC/DMBPE binary mixtures hydrated in excess 1 M NaCl, 10 mM Hepes, and 1 mM EDTA, pH 7.4, recorded at 30 °C in the fluid phase. The magnitude of the scattering vector, q (Å^{-1}), is 2π sin $2\theta/\lambda$, where 2θ is the scattering angle. The composition of the mixtures (in mole ratio) is indicated on the figure.

Table 2: X-ray Repeat Spacings, d_{100}, for DMBPE/DMPC Binary Mixtures Dispersed in 1 M NaCl, 10 mM Hepes, and 1 mM EDTA, pH 7.4, in the Gel (10 °C) and Fluid (30 °C) Phases

DMPC/DMPE (mol/mol)	T (°C)	d_{100} (nm)
100:0	10	5.77
	30	6.62
80:20	10	7.76
	30	7.14
60:40	10	5.07
	30	7.40
50:50	10	4.91
30:70	10	4.84
0:100	10	4.70

DMBPE alone [cf. Swamy et al. (1993)]. From this, it can be concluded that the fluid phase in the first region of the phase diagram in Figure 3 is of the novel isotropic type consisting of aggregated normal micelles (I_{M_I}) that has been characterized for short-chain biotinylphosphatidylethanolamines (Swamy et al., 1993; Swamy & Marsh, 1994). For 50 mol % DMBPE, close to the phase boundary, vestigial traces of lamellar diffraction are observed. This point will be returned to later in the discussion of the ^{31}P NMR spectra.

Spin Label ESR Spectra. The X-ray diffraction data clearly indicate that the gel phases of the DMBPE/DMPC mixtures have a lamellar structure throughout the phase diagram. The characterization of whether these gel phases are of the type with interdigitated lipid chains that are found for hydrated biotinylphosphatidylethanolamines alone (Swamy et al., 1993; Swamy & Marsh, 1994), or are of the normal noninterdigitated type common for hydrated phospholipids

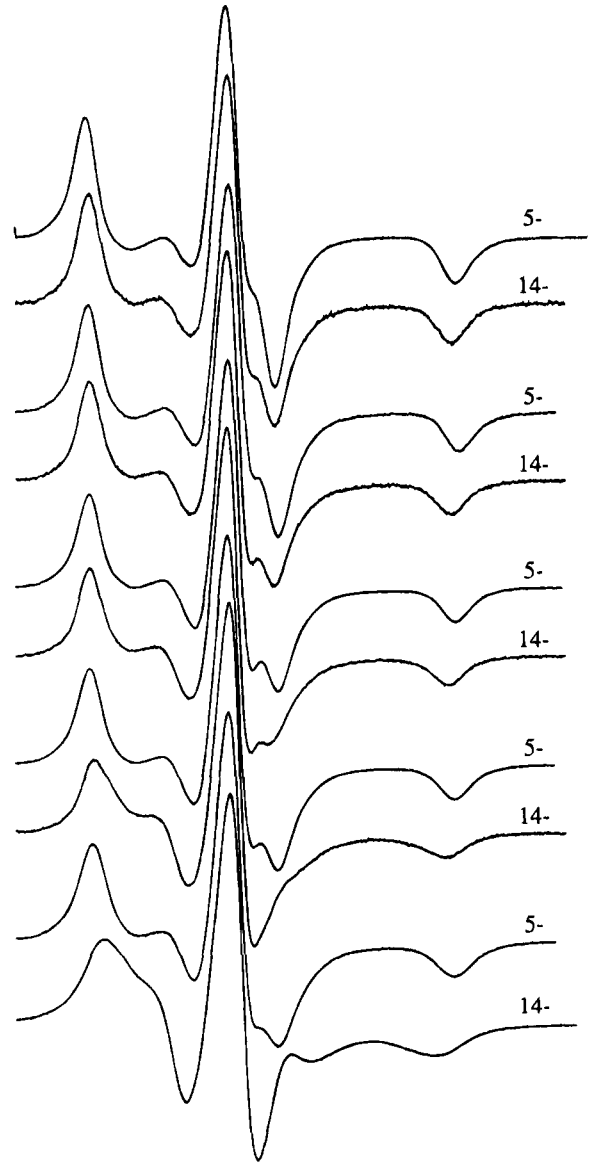

FIGURE 6: ESR spectra of the 5-PCSL and 14-PCSL phospholipid spin label positional isomers in DMPC/DMBPE binary mixtures hydrated in 1 M NaCl, 10 mM Hepes, and 1 mM EDTA, pH 7.4, recorded at 10 °C in the gel phase. The upper spectrum of each pair is from 5-PCSL and the lower from 14-PCSL. From upper to lower, the pairs of spectra refer to DMPC contents in the mixtures of 20, 40, 60, 80, and 100 mol %. Total spectral width = 100 Gauss.

such as DMPC, was based mostly on the values of the repeat spacings. However, as noted previously, a change in the water spacing cannot be completely excluded. Therefore, to support these assignments, the ESR spectra of lipids spin-labeled in their chains close to the polar groups and close to the methyl terminal chain ends have been recorded in the lipid mixtures. By comparing the mobilities of these two sections of the chain, it was possible to detect gel-phase chain interdigitation in biotinyl lipids alone (Swamy & Marsh, 1994).

The ESR spectra of phospholipid probes spin-labelled at the 5- and 14-C atoms of the *sn*-2 chain are given in Figure 6, for different DMBPE/DMPC mixtures at 10 °C in the gel phase. It is seen that, for the lipid mixtures containing up to 60 mol % DMPC, the outer hyperfine splittings in the spectra from the two positions of labeling are very similar. This is in contrast to the ESR spectra from DMPC gel-phase bilayers alone, where the outer hyperfine splitting of 14-PCSL is considerably smaller than that of 5-PCSL. The latter

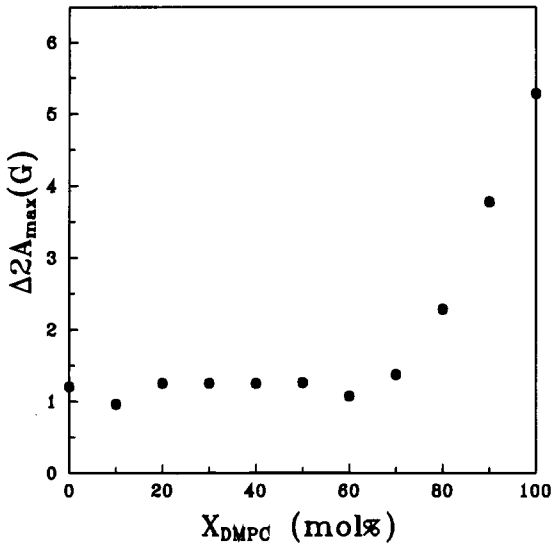

FIGURE 7: Dependence of the difference in outer hyperfine splitting, $\Delta 2A_{max}$, between the ESR spectra from the 5- and 14-PCSL spin labels on composition (mol % DMPC) for DMPC/DMBPE binary mixtures hydrated in 1 M NaCl, 10 mM Hepes, and 1 mM EDTA, pH 7.4, at 10 °C in the gel phase.

is characteristic of the chain flexibility gradient in noninterdigitated gel-phase bilayers, whereas the former behavior is indicative of the greater rigidity of the lipid chains in interdigitated phases [cf. Boggs and Rangaraj (1985) and Bartucci et al. (1993)].

The dependence of the difference in outer hyperfine splittings, $\Delta 2A_{max}$, between the gel-phase spectra of the 5-PCSL and 14-PCSL spin labels on the composition of the DMBPE/DMPC mixtures is given in Figure 7. Comparison of this figure with Figure 3 shows that the value of $\Delta 2A_{max}$ remains very low throughout the first two regions of the phase diagram, indicating that here the gel phase is of the interdigitated type. Beyond this, the values of $\Delta 2A_{max}$ increase rapidly with increasing DMPC content (from 80 mol % onward), indicating that in the third region of the phase diagram the gel phase is not interdigitated. These results fully support the conclusions reached on the basis of the X-ray long spacings. They further indicate that changes in the thickness of the water layer do not make a dominant contribution to the long spacings of the gel phase in the first two regions of the phase diagram.

^{31}P Nuclear Magnetic Resonance. Further characterization of the gel and fluid phases, and confirmation of their identifications made by X-ray diffraction, is offered by broad-line ^{31}P NMR. The proton dipolar decoupled ^{31}P NMR spectra of the hydrated lipid mixtures in the gel and fluid phases are given in Figure 8, panels A and B, respectively. At 10 °C, in the gel phase, the ^{31}P NMR spectra of all lipid mixtures consist of broad, axially anisotropic powder patterns with a chemical shift anisotropy of $\Delta\sigma \approx -54$ to -64 ppm, characteristic of a lamellar gel phase. The smaller absolute value of the effective chemical shift anisotropy corresponds

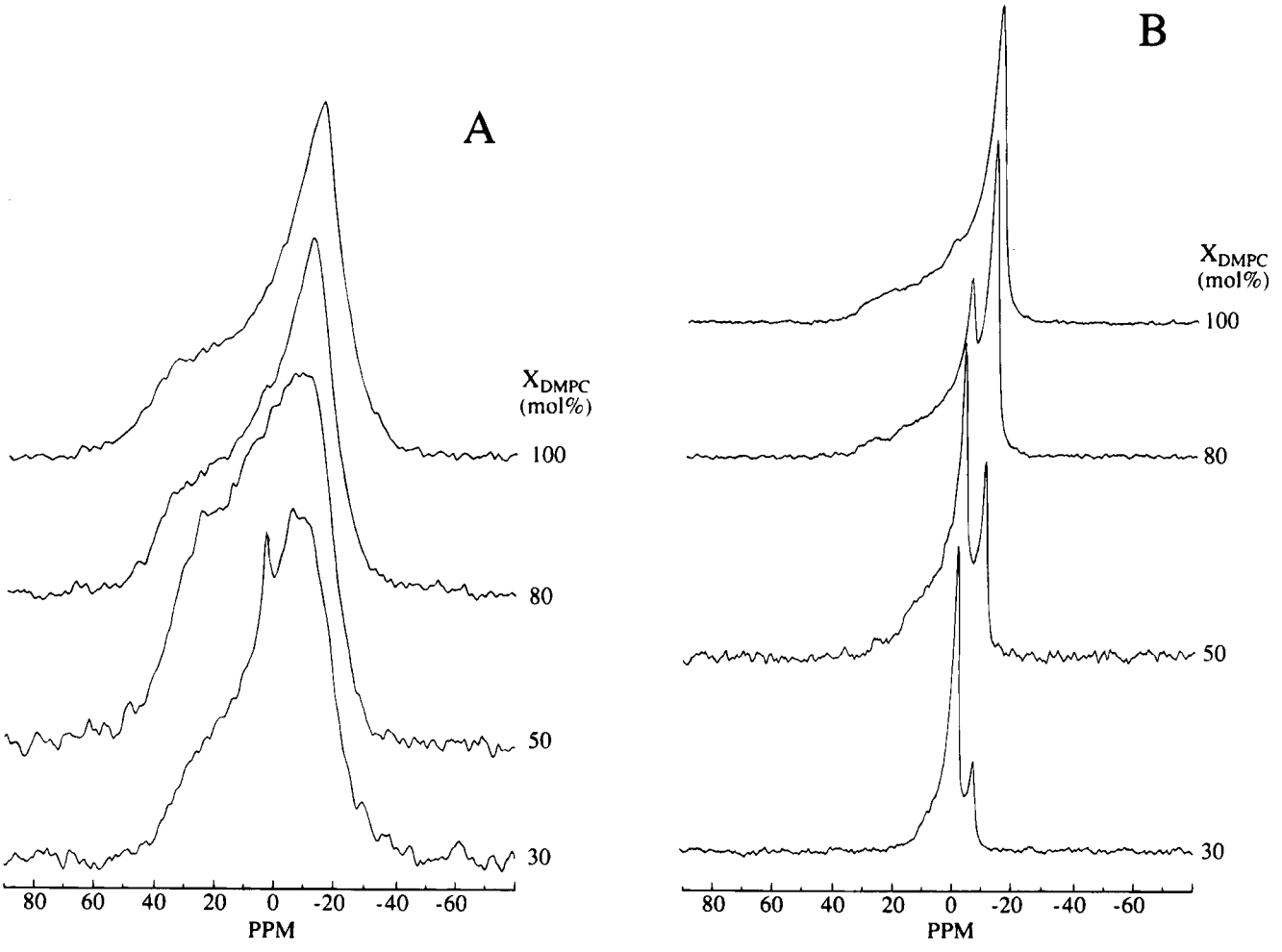

FIGURE 8: Proton-dipolar decoupled 121.5 MHz ^{31}P NMR spectra of DMPC/DMBPE binary mixtures hydrated in 1 M NaCl, 10 mM Hepes, and 1 mM EDTA, pH 7.4, recorded at (A) 10 °C in the gel phase and (B) 30 °C in the fluid phase. Chemical shifts (ppm) are referenced to external 85% phosphoric acid. The composition of the mixtures (mol % DMPC) is indicated on the figure.

to the mixture with 30 mol % DMPC and is similar to that for the gel phase of DMBPE alone (Swamy et al., 1993).

At 30 °C, in the fluid phase, the ^{31}P NMR spectra consist of sharp, axially anisotropic powder patterns. For DMPC alone, a single powder pattern is obtained with chemical shift anisotropy of $\Delta\sigma \approx -49$ ppm, characteristic of the fluid lamellar phase. For the lipid mixtures, the spectra have a second axial powder pattern of smaller chemical shift anisotropy that is superimposed on a powder pattern of larger chemical shift anisotropy. The proportion of the powder pattern with smaller chemical shift anisotropy correlates with the DMBPE content of the mixture. For the mixture with 20 mol % DMBPE, the narrower powder pattern has a chemical shift anisotropy of $\Delta\sigma \approx -26$ ppm, whereas that of the other powder pattern remains reasonably close to that of DMPC alone. Therefore, it can be concluded that in the third region of the phase diagram in Figure 3 the fluid phase has a lamellar structure (i.e., L_α). For long-chain biotinylphosphatidylethanolamines in the L_α phase, it was found that the chemical shift anisotropy was $\Delta\sigma \approx -32$ to -33 ppm (Swamy et al., 1993). Presumably the conformation of the biotinyl headgroup is slightly different in the L_α phase of the lipid mixture, resulting in a somewhat lower chemical shift anisotropy. For the sample with 70 mol % DMBPE, corresponding to the first region of the phase diagram in Figure 3, the chemical shift anisotropy is considerably reduced to $\Delta\sigma \approx -14$ ppm for the narrower component. This unusually low value is similar to that of dipalmitoylbiotinylphosphatidylethanolamine in the fluid I_{M_I} phase (Swamy et al., 1993). This suggests that in the first region of the phase diagram the DMBPE/DMPC mixtures also have this novel structure in the fluid phase, although DMBPE alone gives rise to an isotropic ^{31}P NMR spectrum under these circumstances.

The ^{31}P NMR spectra are therefore in agreement with the identifications of the structures of the various phases of the hydrated DMBPE/DMPC mixtures that were made by X-ray diffraction (at least for the first and third regions of the phase diagram). The temperature dependences of the chemical shift anisotropies deduced from the ^{31}P NMR spectra are given in Figure 9. These yield further information on the structure of the phases of the lipid mixtures, especially for the middle region of the phase diagram. For the mixture with 20 mol % DMBPE, corresponding to the third region of the phase diagram, the behavior is relatively simple. After transition to the fluid phase, the chemical shift anisotropy remains essentially constant with increasing temperature, at values that are consistent with an L_α structure for both DMPC and DMBPE components. For the mixture with 50 mol % DMBPE, the situation is more complex with a multiphasic temperature dependence that is rather similar to that found previously for dipalmitoylbiotinylphosphatidylethanolamine alone (Swamy et al., 1993). Initially on transition to the fluid phase, the chemical shift anisotropy drops to a lower value than that normal for an L_α phase, for both DMBPE and DMPC components. For the DMBPE component, the chemical shift anisotropy, $\Delta\sigma \approx -14$ ppm, is equal to that characteristic for the I_{M_I} phase (cf. above). With increasing temperature in the fluid phase, the chemical shift anisotropy increases for both components, achieving values at 37 °C of $\Delta\sigma \approx -29$ and -45 ppm for the DMBPE and DMPC components, respectively. These values are characteristic of a fluid L_α phase, and the gradual conversion with increasing temperature from the I_{M_I} phase parallels exactly

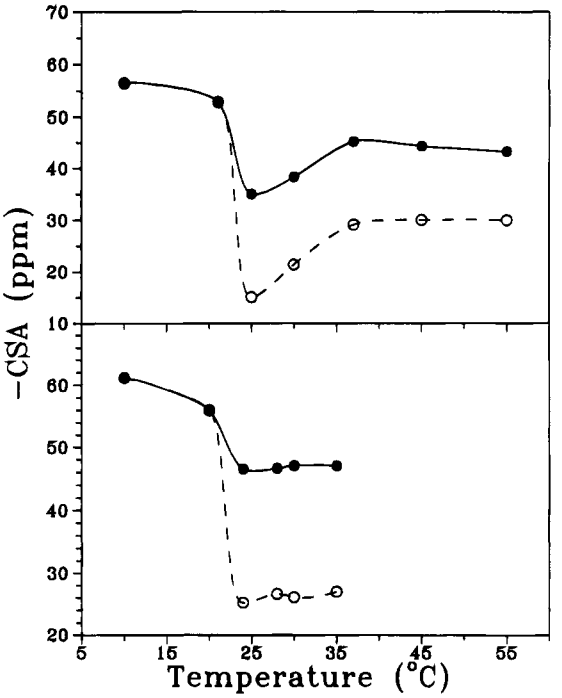

FIGURE 9: Temperature dependence of the apparent chemical shift anisotropy (CSA) in the ^{31}P NMR spectra from DMPC/DMBPE binary mixtures containing 50 mol % (upper) and 80 mol % (lower) of DMPC. The mixtures are dispersed in 1 M NaCl, 10 mM Hepes, and 1 mM EDTA, pH 7.4. Filled symbols are deduced from the powder pattern of the DMPC component and open symbols from the DMBPE component.

that found previously for dipalmitoylbiotinylphosphatidylethanolamine alone under similar circumstances. This behavior correlates with the 50 mol % mixture being at a phase boundary and agrees in this respect with the X-ray diffraction results discussed above (cf. Figure 5). It also supports the identification of the fluid phase in the middle region of the phase diagram as being of lamellar structure (i.e., L_α). In addition, the fact that the DMPC component also displays this unusual temperature dependence implies that both components are miscible in the fluid phase at this composition.

Conclusions. In spite of the rather close chain-melting transition temperatures of DMBPE and DMPC (18.3 and 23.5 °C, respectively), the phase behavior of their hydrated binary mixtures is found to be rather complex. Molecular interactions leading to the formation of different stoichiometric complexes between the two lipids are found in the gel phase. Admixture with DMBPE causes DMPC to take on the rich and unique phase polymorphism exhibited by the biotinyl lipids, for one mixture extending even to that characteristic of a biotinylphosphatidylethanolamine of longer chain length. This demonstrates that surface and polar group modifications can affect the properties of bilayer lipid membranes in dramatic and rather unexpected ways. It is not yet known, for instance, whether such effects may extend to complex membrane glycolipids.

The present experiments were performed in 1 M NaCl to suppress electrostatic effects of the negatively charged biotinyl lipid. In the absence of salt, DMBPE alone also forms an interdigitated gel phase, but the fluid phase is micellar because of electrostatic repulsions between the headgroups and is metastable at low temperature (Swamy et al., 1993). It seems likely that compound formation will take place between DMBPE and DMPC in the gel phase of

binary mixtures, also at low ionic strength. The fluid phase will, however, consist of mixed micelles for part of the phase diagram in the absence of salt.

ACKNOWLEDGMENT

We thank Frau B. Angerstein for synthesis of phospholipids and spin labels.

REFERENCES

Bartucci, R., Páli, T., & Marsh, D. (1993) *Biochemistry 32*, 274−281.

Bayer, E. A., Rivnay, B., & Skutelsky, E. (1979) *Biochim. Biophys. Acta 550*, 464−473.

Boggs, J. M., & Rangaraj, G. (1985) *Biochim. Biophys. Acta 816*, 221−233.

Cevc, G., & Marsh, D. (1987) *Phospholipid Bilayers. Physical Principles and Models*, 442 pp, Wiley-Interscience, New York.

Darst, S. A., Ahlers, M., Meller, P. H., Kubalek, E. W., Blankenburg, R., Ribi, H. O., Ringsdorf, H., & Kornberg, R. D. (1991) *Biophys. J. 59*, 387−396.

Janiak, M. J., Small, D. M., & Shipley, G. G. (1976) *Biochemistry 15*, 4575−4580.

Marsh, D., & Watts, A. (1982) in *Lipid−Protein Interactions* (Jost,P. C., & Griffith, O. H., Eds.) Vol. 2, pp 53−126, Wiley-Interscience, New York.

Rouser, G., Fleischer, S., & Yamamoto, A. (1970) *Lipids 5*, 494−496.

Swamy, M. J., & Marsh, D. (1993) *FEBS Lett. 324*, 56−58.

Swamy, M. J., & Marsh, D. (1994) *Biochemistry 33*, 11656−11663.

Swamy, M. J., Würz, U., & Marsh, D. (1993) *Biochemistry 32*, 9960−9967.

Swamy, M. J., Angerstein, B., & Marsh, D. (1994) *Biophys. J. 66*, 31−39.

Urdal, D. L., & Hakamori, S. (1980) *J. Biol. Chem. 255*, 10509−10516.

Wilchek, M., & Bayer, E. A. (1989) *Trends Biochem. Sci. 14*, 408−412.

Würz, U. (1988) *Prog. Colloid Polym. Sci. 76*, 153−158.

BI9502607